

Sound, infrasound, and sonic boom absorption by atmospheric clouds

Michaël Baudoin and François Coulouvrat^{a)}

Université Pierre et Marie Curie, Institut Jean Le Rond d'Alembert, UMR CNRS 7190, 4 place Jussieu, 75252 Paris cedex 05, France

Jean-Louis Thomas

Université Pierre et Marie Curie, Institut des NanoSciences de Paris, UMR CNRS 7588, 4 place Jussieu, 75252 Paris cedex 05, France

(Received 26 January 2011; revised 24 June 2011; accepted 1 July 2011)

This study quantifies the influence of atmospheric clouds on propagation of sound and infrasound, based on an existing model [Gubaidulin and Nigmatulin, *Int. J. Multiphase Flow* **26**, 207–228 (2000)]. Clouds are considered as a dilute and polydisperse suspension of liquid water droplets within a mixture of dry air and water vapor, both considered as perfect gases. The model is limited to low and medium altitude clouds, with a small ice content. Four physical mechanisms are taken into account: viscoinertial effects, heat transfer, water phase changes (evaporation and condensation), and vapor diffusion. Physical properties of atmospheric clouds (altitude, thickness, water content and droplet size distribution) are collected, along with values of the thermodynamical coefficients. Different types of clouds have been selected. Quantitative evaluation shows that, for low audible and infrasound frequencies, absorption within clouds is several orders of magnitude larger than classical absorption. The importance of phase changes and vapor diffusion is outlined. Finally, numerical simulations for nonlinear propagation of sonic booms indicate that, for thick clouds, attenuation can lead to a very large decay of the boom at the ground level.

© 2011 Acoustical Society of America. [DOI: 10.1121/1.3619789]

PACS number(s): 43.28.Bj, 43.28.Dm, 43.20.Hq, 43.28.Mw [ROC]

Pages: 1142–1153

I. INTRODUCTION

Water droplets in suspensions considerably modify sound propagation. This was first studied by Sewell,¹ who considered only momentum transfers between ambient air and fixed particles. Lamb² modified this model by allowing particle motion. Isakovich³ outlines the importance of heat transfer. Epstein and Carhart⁴ introduce a new formalism to take into account particles elasticity. This work, limited to the low frequency range, is extended by Allegra and Hawley⁵ to emulsions and aqueous suspensions without frequency limitation. This approach, now referred as the ECAH theory, is most suitable for solid particles or emulsions as it cannot take into account phase changes at the particle surface. Viglin⁶ and Oswatitsch⁷ investigate the effects of evaporation and condensation, assuming in a simplified analysis the two phases have the same speed and temperature. This approach is extended by Marble,⁸ Marble and Wooden,⁹ Cole and Dobbins,¹⁰ and Ivandaev and Nigmatulin¹¹ to the case of different speeds and temperatures for the two phases. In particular, a peak of the attenuation per wavelength associated with phase change effects is predicted. Marble and Wooden⁹ and Cole and Dobbins¹⁰ consider a liquid particle surrounded by a mixture of its vapor and an inert gas. The evaporation rate is assumed to be dominated by the diffusion of vapor within the gas. On the contrary, Ivandaev and Nigmatulin¹¹ investigate the case of a liquid droplet in sus-

pension within its vapor only. The evaporation rate is determined by the Hertz–Knudsen–Langmuir formula^{12–14} involving the so-called evaporation coefficient. In all these models, transfers of mass, momentum and energy are modeled by stationary terms. Unsteady effects are included by Gumerov *et al.*¹⁵ for the case of a liquid in suspension within its vapor only. That model is finally extended by Gubaidullin and Nigmatullin¹⁶ to include polydispersed droplets within a gaseous mixture of vapor and inert gas. Duraiswami and Prosperetti¹⁷ show that, when the effects of phase changes on the acoustic wave propagation are maximum, the Knudsen number is necessarily of order one. They therefore propose some corrections to the transfers terms to be taken into account when the droplet size is comparable to the gas mean free path. They also include the presence of an inert gas. However, the model used in the present study is the one of Gubaidullin and Nigmatullin,¹⁶ as it is, to our knowledge, the only one to include simultaneously polydispersion, unsteady effects, mass (evaporation/condensation), momentum and energy surface transfers. It will be shown that the polydispersion plays a major role in the propagation of acoustic waves in clouds, while the Knudsen number remains in practice small enough to neglect the corrections proposed by Duraiswami and Prosperetti.¹⁷

From the experimental point of view, Knudsen¹⁸ is likely the first to have made qualitative observations. Dobbins and Temkin^{19,20} measure attenuation and dispersion in a mixture of oleic acid within nitrogen. However, the frequencies are too large for evaporation and condensation effects to be observed, so that their results are very similar to those of

^{a)}Author to whom correspondence should be addressed. Electronic mail: francois.coulouvrat@upmc.fr

aerosols with solid particles. The influence of phase changes has been measured only in the experiment of Cole and Dobbins in 1971,²¹ performed within a Wilson chamber filled with a water cloud. Droplet concentration is controlled by spark-induced condensation nuclei. The water mass ratio is about 10^{-2} , about 10 times larger than in atmospheric clouds. Concentration and droplet size are controlled optically by Mie diffusion of a light source. Radii range from 1.8 to 10 μm . Sound attenuation is measured through the time decay of a stationary wave at a fixed frequency (80 Hz), and attenuation is plotted versus a dimensionless frequency proportional to the mass ratio. Experimental uncertainty, a 15% error margin very sensitive to optical measurements, is smaller than the mismatch with theory, with experimental attenuation about 35% smaller than in theory. Nevertheless, these experiments remain to our knowledge the only ones measuring quantitatively the influence of phase changes on sound absorption within an aerosol made of water droplets in air.

Since these experiments have been realized, the model¹⁶ has been established with clear theoretical foundations. It is able to handle all effects likely to influence sound propagation in an aerosol of water droplets in air. These effects are, namely, (i) the visco-inertial effects associated to the motion of the droplets relative to the ambient fluid oscillations, (ii) the thermal transfers due to the temperature difference between the gas and the droplets, and (iii) the evaporation/condensation of water, also due to the local disturbance of the thermodynamic equilibrium of the aerosol by the sound field. Phase changes are also affected by (iv) vapor diffusion within dry air, that may limit them by preventing the vapor molecules produced at the droplet surface to diffuse within the air. Hence, the first objective of this paper is to examine the adequacy of Gubaidullin and Nigmatulin's model to predict attenuation of sound and infrasound. We will see in particular that the model is limited to relatively low altitudes (typically less than 4000 m) and low frequency (less than 100 Hz). Then by collecting physical and thermodynamical data for clouds, we will quantify the magnitude of the absorption effect for various types of clouds. Cloud absorption will be compared to classical absorption (due to bulk thermoviscosity and molecular relaxation of nitrogen and oxygen). Finally, a realistic case of application concerning sonic boom propagation will exemplify in a quantitative way the importance of atmospheric clouds.

II. PHYSICAL DATA FOR CLOUDS

In the model, the required physical data about clouds are the mean radius a_0 of the water droplets, the statistical distribution $N(a)$ of droplets size a , the liquid water concentration w_L , the height h of the cloud basis above the ground, and the cloud thickness d . For a given type of cloud, only mean "typical" values are considered. Variability between clouds of the same type is not examined.

Atmospheric clouds are considered as suspensions of almost perfectly spherical liquid water droplets. Only clouds with a small ice content are adequately modeled. Clouds at a temperature higher than 0°C contain only liquid water. In order to freeze at temperatures higher than -40°C , liquid

water needs nuclei in order to initiate the solidification reaction. Water freezes spontaneously only at temperatures below -40°C . In the atmosphere, the number of nuclei is generally insufficient, and a large part of the water remains in the liquid phase. This is the supercooling (or undercooling) phenomenon. Data²² (p. 39) indicate that, between 0°C and -10°C , the liquid water content remains dominant (more than 50%) over the ice content. Hence, the present model is applicable to temperatures higher than approximately -10°C . For ICAO standard atmosphere,²³ this corresponds to altitudes lower than about 3850 m above sea level.

Given this constraint, seven types of clouds observed at altitudes lower than 4000 m have been selected: stratus (fog - ST), altostratus (AS), stratocumulus (SC), early stage cumulus (CE), growing stage cumulus (CG), final stage cumulus (CF) and cumulonimbus (CN). Typical values²² are collected in Table I. Liquid water concentration is measured as w_L in grams of water per cubic meter. These data are only mean, representative values. As many meteorological phenomena, extreme values can be observed from time to time, such as water contents up to 14 g/m^3 for some thunder clouds for instance. The distribution function, where $N(a)da$ is the number of particles per unit volume whose radius lies between a and $a + da$, is given by²² (pp. 26–27):

$$N(a) = Aa^2 \exp(-Ka), \quad (1)$$

where A and K are related to the mean radius, the water content and the liquid water specific mass ρ_{l0} by:

$$a_0 = \frac{\int_0^{+\infty} aN(a)da}{\int_0^{+\infty} N(a)da} \quad \text{and} \quad K = \frac{3}{a_0} \quad \text{and} \quad A = \frac{10^{-3}w_L K^6}{160\pi\rho_{l0}}. \quad (2)$$

III. THE THEORETICAL MODEL

A. Qualitative description of absorption mechanisms

In an atmospheric cloud, droplets (with radius on the order of 10 to 30 μm —see Table I) are in suspension within a gas composed of a mixture of water vapor and air, which itself is a mixture of mostly molecular nitrogen N_2 , molecular oxygen O_2 and argon Ar . At thermodynamic equilibrium, the partial vapor pressure p_v is equal to the saturation pressure $p_{vs}(T)$ given by the Clausius-Clapeyron relation. A sound wave disturbs that equilibrium. In case of an expansion, temperature drops, vapor pressure gets larger than its equilibrium value and, in order to restore equilibrium, some

TABLE I. Physical data for atmospheric clouds.

Type	h (km)	d (m)	w_L (g/m^3)	a_0 (μm)
Fog	0	500	0.05 to 0.5	10
Altostratus	2.0 to 4.5	2000	0.2 to 0.5	20
Stratocumulus	0.6 to 2.0	800	0.1 to 0.5	20
Cumulus				
Early stage	0.5 to 2.0	500	0.2 to 0.5	10
Growing stage	0.5 to 2.0	1500	0.5 to 1.0	20
Final stage	0.5 to 2.0	2500	0.5 to 3.0	30
Cumulonimbus	0.5 to 2.0	5000	0.5 to 3.0	30

vapor has to condense. That phase change requires some energy under the form of latent heat, that is pumped from the acoustical wave. A spectacular illustration of this effect is seen on some photographs of condensation clouds taking the form of a Mach cone around aircraft flying supersonically at low altitudes. Similarly, a compression wave induces a partial vaporization of the water droplets. However phase changes are not instantaneous. For high frequencies, the cloud cannot adapt to the fast temperature changes and it appears as “frozen” in its initial thermodynamic state. On the contrary, for low frequencies, the cloud always remains at thermodynamic equilibrium, and no sound absorption is induced. Hence, sound absorption due to phase changes is most efficient in some intermediate frequency range. We will see the critical frequency is around 0.1 Hz, a value controlled simultaneously by vapor diffusion, and by water mass concentration. Indeed phase changes occur at the surface of the droplets. A strong evaporation may induce a surface accumulation of vapor molecules that also need time to diffuse within the ambient air to restore an equal spatial repartition. The second effect that may affect sound propagation is momentum transfers between the droplets and the gas. Indeed, a particle relative motion within a fluid induces a viscous drag that dissipates part of the energy producing that motion. Acoustic motion being unsteady, it also induces an inertial Archimedes force on the droplet that contributes to the velocity mismatch between the air and the liquid, and hence to the viscous drag. Finally, droplets and air have different thermal properties and do not adapt in phase to the acoustical temperature. Hence a temperature mismatch occurs, that leads to a dissipative heat flux. Because phase changes are controlled by temperature, mass and heat transfers at the surface of water droplets are strongly coupled to one another.

B. Outline of the model

The two-phase model of Gubaidulin and Nigmatulin¹⁶ is obtained by spatial averaging of Navier-Stokes equations over a characteristic volume containing a large number of particles, but nevertheless small enough compared to the acoustic wavelength. Similar equations can be obtained by performing temporal²⁴ or statistical²⁵ average. Mass, momentum and energy conservation equations are obtained for each phase (liquid and gas), with an additional equation required to describe the mass conservation of vapor. The necessary following conditions are to be fulfilled. (1) The average of products of fluctuation (the so-called pseudoturbulence) is neglected. (2) Gravity is neglected and there is no heat source. (3) The liquid droplets are supposed to be rigid. (4) The momentum exchanged during phase change is neglected. (5) The suspension is dilute.

$$\frac{\partial(\alpha_g \rho_g)}{\partial t} + \nabla \cdot (\alpha_g \rho_g \mathbf{v}_g) = -J, \quad (3)$$

$$\frac{\partial(\alpha_l \rho_l)}{\partial t} + \nabla \cdot (\alpha_l \rho_l \mathbf{v}_l) = -J, \quad (4)$$

$$\rho_{lo} \frac{\partial(\alpha_l)}{\partial t} + \rho_{lo} \nabla \cdot (\alpha_l \mathbf{v}_l) = J, \quad (5)$$

$$\alpha_g \rho_g \frac{d_g v_g}{dt} = -\mathbf{F} - \nabla p_g + \nabla \cdot \Sigma, \quad (6)$$

$$\alpha_l \rho_{lo} \frac{d_l v_l}{dt} = \mathbf{F}, \quad (7)$$

$$\alpha_g \rho_g C_{go}^p \frac{d_g T_g}{dt} = Q_g + \chi_{go} \nabla^2 T + \Sigma : \mathbf{D}, \quad (8)$$

$$\alpha_l \rho_{lo} C_{lo} \frac{d_l T_l}{dt} = Q_l, \quad (9)$$

$$Q_g + Q_l = -Jl_o. \quad (10)$$

Equations (3)–(5) formulate, respectively, the mass conservation of the gaseous, vapor, and liquid phases, Eqs. (6) and (7) the momentum conservation of the gaseous and liquid phases, and Eqs. (8) and (9) the conservation of energy of the gaseous and liquid phase. Equation (10) is the energy balance at the surface of the droplets. The subscripts $k = a, g, l, v$ designate, respectively, the dry air (inert gas), the gaseous (vapor + dry air) phase, the liquid phase and the vapor. The subscript “o” is used for constant parameters, α_k is the volume fraction occupied by phase k , with the relation $\alpha_g + \alpha_l = 1$. Notations $\rho_k, T_k, \mathbf{v}_k, p_k$ are, respectively, for the average density, temperature, velocity and pressure of phase k , while $d_k/d_k = \partial/\partial t + \mathbf{v}_k \cdot \nabla$ is the convective derivative associated to the motion of phase “k.” Then $\mathbf{v} = \alpha_g \mathbf{v}_g + \alpha_l \mathbf{v}_l$, $T = \alpha_g T_g + \alpha_l T_l$ and $\mathbf{D} = 1/2(\nabla \mathbf{v} + \nabla \mathbf{v}^T)$ are, respectively, the average velocity, temperature and deformation rate tensor of the suspension. The viscous stress tensor of the suspension is $\Sigma = 2\mu_{go} \mathbf{D} + (\zeta_{go} - 2\mu_{go}/3)(\nabla \cdot \mathbf{v})\mathbf{I}$, and $\mu_{go}, \zeta_{go}, C_{go}^p$, and χ_{go} represent the dynamic shear and bulk viscosity of the gaseous phase, its heat capacity at constant pressure, and its heat conductivity. C_{lo} and l_o are the heat capacity of the liquid phase and the latent heat of evaporation. Finally, J, \mathbf{F}, Q_g , and Q_l denote the mass flux induced by phase change, the average force applied on the particles, the heat flux from the gaseous phase toward the interface and the heat flux from the liquid phase toward the interface. Note that only vapor diffusion linked to surface effects of evaporation and condensation is taken into account, while the one due to pressure and temperature bulk gradients induced by the acoustical wave is neglected. Since the suspension is polydisperse, the velocity and temperature field of the liquid phase can be seen as some averages (over the different particle sizes) of the velocity and temperature of droplets of a given size a : $\mathbf{v}_p(a, \mathbf{x}, t)$ and $T_p(a, \mathbf{x}, t)$. Thus, we have $\mathbf{v}_l = \langle \mathbf{v}_p(a, \mathbf{x}, t) \rangle_a$ and $T_l = \langle T_p(a, \mathbf{x}, t) \rangle_a$, where $\langle f \rangle_a = (1/\alpha_{lo}) \int_0^{+\infty} (4/3\pi a^3) f(a) N(a) da$ is the average over the different particle radii of function $f(a)$.

To describe the propagation of a plane sound wave of angular frequency ω , these equations are written in a 1D geometry, expressed in the Fourier space and linearized around thermodynamic equilibrium (defined by the variables $\alpha_{go}, \alpha_{lo}, \rho_{go}, \rho_{vo}, \mathbf{v}_{go} = \mathbf{v}_{lo} = 0, T_{go} = T_{lo} = T_o$ and p_{go} , which are the equilibrium counterparts of previously defined variables).

Each gaseous species satisfies the ideal gas law $p_k = \rho_k R_k T_g$ with $k = v, a$ and R_k is the ideal constant of gas k . The total pressure is the sum of the partial ones (Dalton’s

law) $p_g = p_v + p_a$. Gas total mass is the sum of its components $\rho_g = \rho_v + \rho_a$. The saturation vapor pressure p_{vs} satisfies the Clausius-Clapeyron relation, with T_Σ the temperature at the droplet surfaces:

$$T_\Sigma(dp_{vs}/dT_\Sigma) = \rho_v l_o. \quad (11)$$

Closure is achieved by providing adequate expressions for the mass, momentum and heat transfers (respectively, J , \mathbf{F} , Q_l , and Q_g) between gas and liquid. Since the droplets are small and their motion relatively slow, the Reynolds number associated with the droplet motion is small, so that the force applied on a single droplet can be computed from linear Stokes equations. For an unsteady motion, this force is the sum of the Stokes, Basset, Added mass and Archimedes forces.²⁶ The first term is the classic Stokes drag applied on a sphere embedded in a steady viscous flow. The Basset hereditary force is an unsteady viscous term due to the time required by the viscous diffusion layer to adapt to new boundary conditions. The added mass term is linked to the inertia of the liquid, which must be displaced when a sphere is accelerated or decelerated. The Archimedes force is an unsteady inertial force which comes from the difference of density between the particles and the surrounding medium. The following expression is obtained in the Fourier space:

$$\mathbf{F} = \alpha_{lo} \rho_{lo} \left\langle \frac{\mathbf{v}_g - \mathbf{v}_p}{\tau_v^*} - \frac{\mathbf{v}_g}{\tau_A^*} \right\rangle_a \quad (12)$$

where τ_v^* is a complex time associated to the sum of Stokes, Basset, and Added mass terms, and τ_A^* is a complex time associated to Archimedes force (defined below).

Heat flux expressions in the gas and liquid phases are obtained by solving the unsteady heat equation inside and outside the droplet with a surface temperature T_Σ :

$$Q_g = -\alpha_{lo} \rho_{lo} r_o C_{go}^p \left\langle \frac{T_g - T_\Sigma}{\tau_{\Sigma_g}^*} \right\rangle_a, \quad (13)$$

$$Q_l = -\alpha_{lo} \rho_{lo} C_{lo} \left\langle \frac{T_l - T_\Sigma}{\tau_{T_l}^*} \right\rangle_a, \quad (14)$$

with $\tau_{\Sigma_g}^*$ and $\tau_{T_l}^*$ the complex characteristic times associated with heat conduction in the gas and liquid, respectively, and r_o the ratio of densities $r_o = \rho_{go}/\rho_{lo}$.

Expression of the mass flux is obtained by equating the flux of evaporation given by Hertz-Knudsen-Langmuir formula J_β , to the flux of diffusion of vapor through the air $J = J_\beta = J_d$ with:

$$J_\beta = \alpha_{lo} \rho_{lo} \frac{r_o}{p_{go}} \left\langle \frac{p_v - p_\Sigma}{\tau_\beta} \right\rangle_a, \quad (15)$$

$$J_d = \alpha_{lo} \rho_{lo} \frac{r_o}{p_{go}} \left\langle \frac{p_\Sigma - p_{vs}}{\tau_D^*} \right\rangle_a, \quad (16)$$

with p_Σ the vapor pressure reached after evaporation and before diffusion in the inert gas, τ_β the real time associated

with phase change and τ_D^* the complex time associated with diffusion through the air.

The times appearing above are defined by the following formula. Times marked with a superscript “*” are complex times. The notation τ is used for steady transfers, and the notation θ for unsteady transfers.

Times associated with

- Momentum transfers

$$\left. \begin{aligned} \tau_v &= \frac{2 \rho_{lo} a^2}{9 \rho_{go} \nu_{go}} & \theta_v &= a^2/\nu_{go} \\ \tau_v^* &= \tau_v / \left[1 - \frac{1}{9} i \omega \theta_v + \frac{1-i}{\sqrt{2}} \sqrt{\omega \theta_v} \right] & \tau_A^* &= -i/(\omega r_o) \end{aligned} \right\} \quad (17)$$

In τ_v^* , the three terms correspond, respectively, to Stokes, Added mass and Basset force (with τ_v associated with steady Stokes drag), and τ_A^* is associated with Archimedes force.

- Heat transfers in the gaseous phase

$$\left. \begin{aligned} \tau_T &= \frac{1}{3} \frac{\rho_{lo} a^2}{\rho_{go} \kappa_{go}} & \theta_{T_g} &= a^2/\kappa_{go} & z_g &= e^{-i\pi/4} \sqrt{\omega \theta_{T_g}} \\ \eta_g &= \frac{1}{1+z_g} & \tau_{T_g}^* &= \frac{1}{3} \theta_{T_g} \eta_g & \tau_{\Sigma_g}^* &= \frac{\alpha_{lo}}{\alpha_{go}} \tau_{T_g}^* \end{aligned} \right\} \quad (18)$$

with τ_T the time associated with steady heat transfers without phase change

- Heat transfers in the liquid phase

$$\left. \begin{aligned} \theta_{T_l} &= a^2/\kappa_{lo} & z_l &= e^{-i\pi/4} \sqrt{\omega \theta_{T_l}} \\ \eta_l &= \frac{5[3z_l(3+z_l^2)th(z_l)]}{z_l^2(th(z_l) - z_l)} & \tau_{T_l}^* &= \frac{1}{15} \theta_{T_l} \eta_l \end{aligned} \right\} \quad (19)$$

- Vapor diffusion in air

$$\left. \begin{aligned} \tau_D &= \frac{1}{3} \frac{\rho_{lo} a^2}{\rho_{go} D} & \theta_D &= a^2/D & z_D &= e^{-i\pi/4} \sqrt{\omega \theta_D} \\ \eta_D &= \frac{1}{1+z_D} & \tau_D^* &= \frac{1}{3} \frac{R_v}{R_g} (1 - k_{vo}) \theta_D \end{aligned} \right\} \quad (20)$$

with τ_D the time associated with steady vapor diffusion

- Evaporation/condensation

$$\tau_\beta = \frac{1}{3} \sqrt{\frac{2\pi \gamma_k c_{vo} a}{\gamma_v \beta c_{go}^2}}. \quad (21)$$

The two parameters $m = \alpha_{lo} \rho_{lo} / \alpha_{go} \rho_{go}$ and $k_{vo} = \rho_{vo} / \rho_{go}$ are the most important ones that influence the magnitude of the attenuation induced by the suspension. The attenuation induced by viscoinertial and thermal effects is directly linked to the quantity of droplets present in the suspension and thus to the mass fraction m , while the phase change effects are directly related to the quantity of vapor k_{vo} . In the above expressions, $\nu_{go} = \mu_{go} / \rho_{go}$ is the gas kinematic viscosity, $\kappa_{lo} = \chi_{lo} / \rho_{lo} C_{lo}$ and $\kappa_{go} = \chi_{go} / \rho_{go} C_{go}^p$ are the thermal diffusivity of the liquid and gaseous phases, respectively, D the binary diffusion coefficient of vapor in air, γ_k the heat capacity ratio of phase k , c_{vo} and c_{go} the sound speeds in

vapor and in the gaseous phase, respectively, and β is the evaporation parameter. We can note that τ_v , τ_T , and τ_D on one hand, and θ_v , θ_T , and θ_D on the other hand, share similar written forms. This comes out from the fact that each time arises from the solution of an unsteady diffusion equation (Stokes, heat or diffusion equation). The only difference is that Stokes equation being a vectorial equation, a factor $2/9$ instead of $1/3$ appears in the expression of τ_v . Complex times τ^* are also similar, but an additional term (the added mass) appears in the expression of τ_v^* . To each time, we can associate a characteristic frequency. We note $f_v = 1/(2\pi\tau_v)$ the frequency of steady momentum transfers, and $f_{pc} = m/(2\pi\tau_D)$ the frequency associated with phase changes. Expression of τ_D^* involves the coefficient $(1 - k_{vo})$, which shows that, in the mass diffusion processes, only gradient concentrations are taken into account. Thermodiffusion, e.g., mass diffusion induced by temperature gradients (Soret effect), is neglected as it is known to be of a smaller order of magnitude. Finally, the expression for the dispersion relation is detailed in the Appendix.

For atmospheric application, the model has to be complemented by data for the dependence of various coefficients with pressure and temperature down to -10°C . Most of them are in Ref. 22. The saturation pressure $p_{vs}(T)$ follows Magnus formula (p. 854) in the temperature range $[-50^\circ; +50^\circ\text{C}]$. Two different expressions for specific heat of liquid water C_{lo} are given (p. 93), either in the range $[-4.2^\circ; +35^\circ\text{C}]$, or in the range $[-37.0^\circ; -4.2^\circ\text{C}]$. For density of liquid water ρ_{lo} , two formula can be found pp. 87, in the range either $[0^\circ; 100^\circ\text{C}]$ or $[-33^\circ; 0^\circ\text{C}]$. Expression for vapor diffusion coefficient D is found pp.503. Evaporation latent heat l_o satisfies Kirchhoff formula (pp. 116). Heat conductivity of vapor χ_{vo} , of dry air χ_{ao} and of the gaseous mixture χ_{go} can all be found p. 508. Ref. 27 provides thermal conductivity of liquid water χ_{lo} , and the specific heat at constant pressure C_{vo}^p and ratio of specific heat γ_v of vapor. Data are extrapolated by a second order polynomial to negative temperatures. Sound speed is deduced by the formula for perfect gases $c_{ko} = \sqrt{\gamma_k R_k T}$. Molar mass is 18 g/mol for vapor and 28.966 g/mol for dry air. Classical formulae to obtain γ_g , R_g , and C_g^p as an ideal mixture of dry air and vapor are used. Given the very low vapor concentration, gas viscosity is identified as that of dry air, following the well-known Sutherland formula.

C. Critical discussion on the model assumptions

The model is limited by a number of various approximations that need a closer examination. The *low frequency* approximation allows to view the cloud as a homogeneous medium at the acoustic wavelength scale $\lambda \gg a_0$. It also enables us to consider the gas locally incompressible at the droplet scale a , so that we can use the classical expression Eq. (12) for the momentum transfer. We are presently interested in the infrasonic and low audible frequency range, lower than 100 Hz (this upper limit value is fixed by another model limitation), which gives a ratio $a/\lambda < 10^{-5}$, indeed very small.

In the *dilute approximation*, interactions between droplets are neglected when estimating the transfers terms.

It yields expressions *linear* with particle concentration α_{lo} . Estimating the volume fraction occupied by the liquid water gives $\alpha_{lo} = w_L/\rho_{lo} = 3 \times 10^{-6} \ll 1$. Interactions associated with high concentration of rigid scatterers generally begin to be significant for volume fractions of order 1%, four orders of magnitude larger than the present one. Note the present model (without heat and mass transfers) has been extended to concentrated suspensions of rigid particles^{28,29} and compared favorably to experiments for suspensions of nanoparticles in water in the ultrasonic frequency range.

For the *continuum approximation*, Ref. 17 examines wave propagation in fogs in the intermediate regime of Knudsen number Kn of order 1, that maximizes the mass exchanges through evaporation and condensation. This transitional regime between the continuum limit (presently considered) and the free molecular limit ($\text{Kn} \gg 1$) is treated by introducing finite Knudsen corrections to the exchange terms (like Stokes viscous drag or heat flux). However, given values of Table I, we can estimate the Knudsen number for atmospheric clouds to be $\text{Kn} = \mu_{go}/\rho_{go}c_{go}a = 0.0042$ at the ground level ($\rho_{go} = 1.2$ kg/m³, $\mu_{go} = 1.7 \times 10^{-5}$ Pa s and $c_{go} = 340$ m/s) for the smallest droplets, and $\text{Kn} = 0.0062$ at 4000 m altitude. Hence, the approximation of *small Knudsen number* is very realistic for atmospheric clouds.

According to the *linear approximation*, transfer terms are modeled by linear expressions in terms of velocity, pressure or temperature mismatches, which implies a slow flow motion, or a *small Reynolds number* (Stokes flow). For an acoustical wave of amplitude P_0 , the Reynolds number can be estimated to be $\text{Re} = P_0 a / \mu_{go} c_{go}$. For a sonic boom at the ground level with typical Concorde amplitude of 50 Pa (100 Pa with pressure doubling due to ground reflection), this gives a value $\text{Re} = 0.26$, smaller than unity. However, this estimation of the Reynolds number is quite conservative, as it assumes the velocity mismatch between the droplets and the ambient gas is of the same order as the gas velocity itself. This was for instance the erroneous assumption of Sewell's model¹ considering fixed particles. In reality, droplets are convected by the gas, only a small part of the wave field is absorbed, and the velocity mismatch is only a small fraction of the gas velocity. So, for most acoustical applications, including sonic boom, the small Reynolds number assumption is well satisfied. However, for very intense sound field like blast nearfields, amplitudes can reach several thousand Pascals, and that assumption should be examined more carefully. Concerning thermal effects, the conclusion is similar, as both air and water Prandtl numbers are of order one.

The last approximation considers liquid droplets as rigid bodies, and air as a *perfect gas*. The assumption of liquid water as almost incompressible for an aerial acoustic wave is perfectly satisfied because of the very large impedance contrast between air and liquid water (the ratio is about 2.8×10^{-4}). On the contrary, the second approximation is much more constraining. Indeed, at audible frequencies, absorption of acoustic wave is dominated by real gas effects, namely, the vibrational relaxation of diatomic molecules of nitrogen N_2 and oxygen O_2 that make about 99% of the mass of the air.³⁰ Relaxation frequencies of nitrogen in air saturated with water vapor (100% relative humidity) are typically

of one or several hundreds of Hz, depending on temperature.³¹ The quantitative comparison between cloud and classical sound absorption will show that sound absorption in clouds is dominant by several orders of magnitude over the classical one for infrasonic and low audible frequencies, up to typically 100 Hz. However for higher frequencies, the two sources of absorption turn out of the same order of magnitude. Hence real gas effects cannot be neglected anymore in the frequency range 100 Hz to 1 kHz. In order to be applicable in this frequency range, the model should be modified to include real gas effects for dry air. For frequencies higher than 1 kHz, oxygen relaxation and classical thermoviscous effects are dominant, and the effect of water droplets gets negligible. At still higher frequencies there may be droplet resonances also.

IV. SOUND AND INFRASOUND ABSORPTION

A. Mechanisms of sound absorption

The main unknown in the data used in the model is the value of the evaporation coefficient β . This parameter (which appears in Hertz–Knudsen–Langmuir formula) represents the proportion of vapor molecules which condense when impacting the interface. Note that various improvement of the Hertz–Knudsen–Langmuir formula exist (see Schrage¹⁴ and Barrett and Clement¹²) and rely on different assumptions about the Maxwellian distribution of vapor molecules close to the interface. Concerning the experimental determination of the parameter β , large differences are reported in the literature, from $\beta = 0.01$ to $\beta = 1$ (for a review see Eames *et al.*¹³). Such discrepancies are likely due to differences in the various experimental processes, especially in the measurement of the surface temperature T_Σ . Recent results¹³ for pure water evaporating into a space containing only water vapor, indicate that the true evaporation coefficient is likely to be unity, and is anyway larger than 0.5. However, under real conditions for atmospheric clouds with a gaseous mixture and chemical impurities at the droplet surface, this value may be significantly lower. The question then arises whether this uncertain value significantly influences sound absorption in clouds, as evaporation/condensation is known to be dominant at low frequencies. Hence sound absorption has been computed (Fig. 1) in the frequency range [0.01 Hz – 10

kHz]. The lower value is chosen well above the acoustic cut-off frequency (typically 3.3 mHz) resulting from gravity. Realistic conditions for clouds have been selected regarding their variability according to Table I. These conditions are $a_0 = 10 \mu\text{m}$ for a monodisperse suspension, $w_L = 1 \text{ g/m}^3$ for an altitude of 2000 m ($T_0 = 2^\circ\text{C}$, $p_{go} = 794 \text{ hPa}$). Four values of the evaporation coefficient have been retained: 1 (theoretical maximum and likely value in ideal conditions), 0.1, 0.01 (lowest value reported in the literature) and 0 (no evaporation effect). Clearly the figure shows that, as soon as evaporation/condensation is taken into account, it is the dominant effect for (infrasonic) frequencies lower than 10 Hz. Viscous and other thermal effects are dominant only for higher (audible) frequencies. Moreover, the sound attenuation rate is almost the same for $\beta = 0.1$ and $\beta = 1$. In this range, the phenomenon is limited not by the rate of evaporation of molecules at the droplet surface, but by the bulk diffusion of vapor molecules within the gas mixture. Even in the case $\beta = 0.01$, precise values of the absorption coefficient are modified, but their magnitude order keeps the same (between 0.1 and 1 dB/km in the frequency range 0.02 to 10 Hz). Hence, all present conclusions about the importance of sound absorption and evaporation/condensation effects will remain valid, whatever the precise value of the evaporation parameter. Since most recent results suggest β is close to one, and given the weak variations of sound absorption for values of β above 0.1, subsequently we chose $\beta = 1$.

The relative importance of the various absorption mechanisms is now discussed. In the same conditions as for Fig. 1, the absorption coefficient (Fig. 2) and phase velocity (Fig. 3) are displayed versus frequency. The relative importance of the various mechanisms involved is compared, by taking into account only viscous effects, thermal and viscous effects without phase changes, or all effects altogether. Note it is impossible to isolate phase change effects, as they are intimately coupled to thermal ones. Once again, one observes that evaporation and condensation mechanisms (controlled by diffusion) are dominant at low frequencies, with dispersion effects most sensitive below the characteristic frequency of phase change $f_{pc} \approx 0.1 \text{ Hz}$. Thermal and viscous effects are important only above 10 Hz, slightly below the characteristic frequency of steady viscous effects f_v , which is here about 121 Hz at the ground level. We will see later that

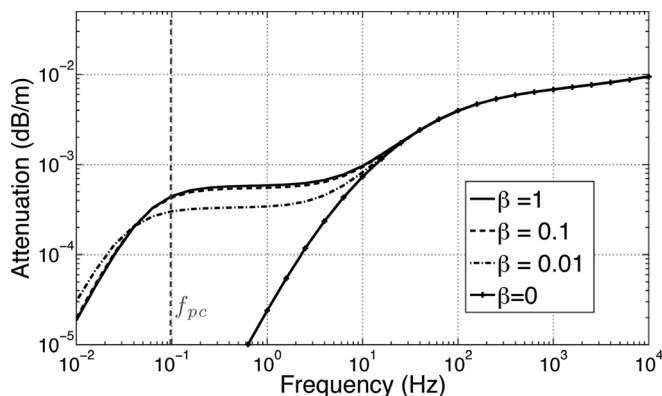


FIG. 1. Influence of the evaporation coefficient parameter on absorption by clouds ($a_0 = 10 \mu\text{m}$, $w_L = 1 \text{ g/m}^3$, $T_0 = 2^\circ\text{C}$, $p_{go} = 794 \text{ hPa}$).

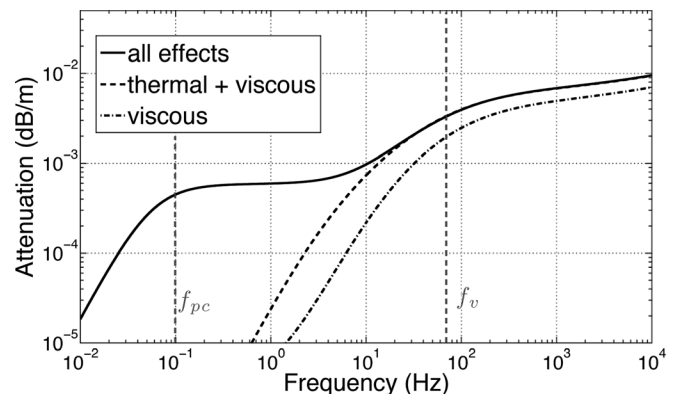


FIG. 2. Influence of various effects on absorption by clouds.

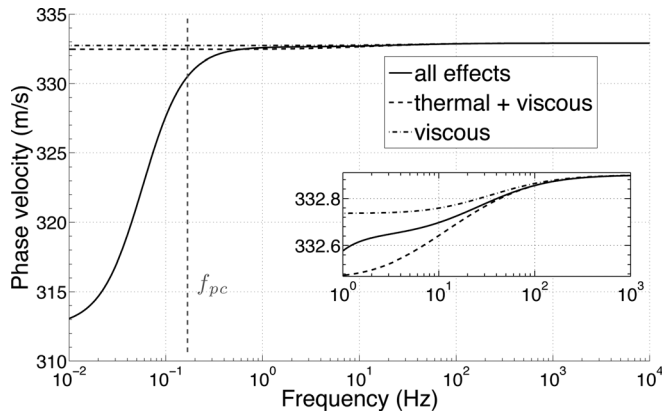


FIG. 3. Influence of various effects on sound speed in clouds.

f_{pc} and f_v are related to one another by $f_{pc} \approx mf_v$ where $m \approx 10^{-3} w_L / (\alpha_{go} \rho_{go})$ is the mass fraction, typically of order 10^{-3} for clouds. Unsteady effects (like Basset history force) play a significant role only at higher frequencies (around 1000 Hz). However, in this high frequency range, real gas effects are anyway dominant. Hence, in any case, unsteady effects are unlikely to play a significant role for absorption of sound in clouds. However, it is an important mechanism to take into account in other cases of suspensions, like solid nanoparticles in water for instance.³² Viscous and thermal effects have similar behavior with frequency because the Prandtl number of air is close to one, and they are comparable in amplitude.

Thermal and viscous effects introduce very small dispersion, contrarily to phase changes that strongly diminish (by up to 6%) the sound speed at frequencies lower than 1 Hz. Indeed, the effective sound speed is $c_{\text{eff}} = 1 / \sqrt{\xi_{\text{eff}} \rho_{\text{eff}}}$ where ρ_{eff} is the effective density and χ_{eff} the effective compressibility. For frequencies $f \gg f_{pc}$, phase changes are frozen, because they are slow compared to acoustic variations. Then, only thermal and viscous exchanges modify the effective density and compressibility of the medium by the introduction of high density and weakly compressible particles. However, these effects are small since they are proportional to the quantity m of liquid present in the suspension, which is small for an atmospheric cloud (see the zoom on Fig. 3). For frequencies $f \ll f_{pc}$, the medium behaves like an effective medium with instantaneous phase changes. In this case, Landau and Lifshitz³³ have shown that the presence of liquid droplets can result into a large effective sound speed decrease. Such variations occur even for a vanishingly small quantity of liquid. This decrease is a consequence of a modification of the thermodynamic behavior of the gaseous phase in the presence of its condensed counterpart. While this effect remains smaller than the one induced by the presence of vapor bubbles in a liquid, it can result into a 10% drop of the sound speed for a suspension of liquid droplets surrounded by its vapor at atmospheric pressure and temperature of 100°C. The results of Landau, valid for a liquid surrounded by its vapor, have been extended recently³⁴ in the presence of a neutral gas. The decrease of the sound speed observed in Fig. 3 is consistent with these theoretical predictions.

Two different characteristic times may influence phase change effects: The characteristic time τ_β for the process of evaporation and condensation at the droplet surface, and the characteristic time τ_D for vapor diffusion within air. The first one is very small, on the order of 10^{-8} s, corresponding to frequencies of several MHz. This explains why the present results are quite insensitive to the value of the evaporation coefficient β . In the considered frequency range, phase changes are almost instantaneous. The characteristic time for thermal effects is $\tau_T = \rho_{lo} C_p^l a^2 / 3 \chi_g$. Its ratio to the characteristic time for steady viscous effect τ_v is equal to $3Pr/2$. As the Prandtl number of air Pr is of order one, both are of the same orders of magnitude. The ratio τ_D/τ_v is equal to $3Sc/2$ where $Sc = \mu_g / \rho_{g0} D$ is the Schmidt number, also of order one for air and vapor. As demonstrated theoretically^{9,10} and experimentally²¹ in a liquid/gas mixture, there are two coupled thermal modes. The first one (fast mode) is pure *thermal* diffusion. If energy is brought to the medium through a compression, the ambient gas heats, following the state equation. That heating is transmitted through liquid particles by thermal diffusion, hence its dynamic is governed by τ_T . The slow mode induces phase changes. After gas compression and heating, the vapor pressure p_v differs from saturation pressure p_{vs} which has increased through heating. Vapor pressure has to be increased to recover equilibrium, which implies that part of the liquid will vaporize (which is almost instantaneous) and then diffuse. This now induces a *decrease* of the ambient gas and liquid temperatures to pump the necessary latent heat. For this mode, the source of the dynamic relaxation process is the liquid. If the liquid mass concentration is small, that process will be much slower because it is necessarily proportional to the small quantity of liquid present in the suspension (contrarily to the first mechanism which is a transfer of heat from the gas, that is overwhelming relative to the liquid). In this case the characteristic time is τ_D/m . For clouds, m is typically of order 10^{-3} , hence the characteristic frequency of phase change $f_{pc} = m / (2\pi\tau_D) = (3Sc/2)mf_v \approx mf_v$, is about 0.1 Hz. Around this frequency, attenuation per wavelength reaches a maximum value, and the frequency behavior of the coefficient of absorption changes, from a quadratic growth below f_{pc} to a plateau value above.

B. Influence of cloud physical parameters

The absorption coefficient in clouds, being governed by phase change effects at low frequencies, and viscous drag at higher ones, tends to increase with the total mass of water for a given droplet radius (here $a = 10 \mu\text{m}$): the increase in the number of sound absorbers increases sound absorption. This is observed on Fig. 4 in the frequency range 0.1 Hz to 10 kHz, where the water content w_L takes three realistic values ranging from 0.5 to 3.0 g/m³. However, while the characteristic frequencies of thermal and momentum exchanges are not affected by the water content, the frequency of phase change f_{pc} is directly proportional to the liquid content. Thus, when the water content is decreasing, the characteristic frequency is also decreasing. Clouds with low water content hence have a plateau value of lower amplitude but of wider frequency

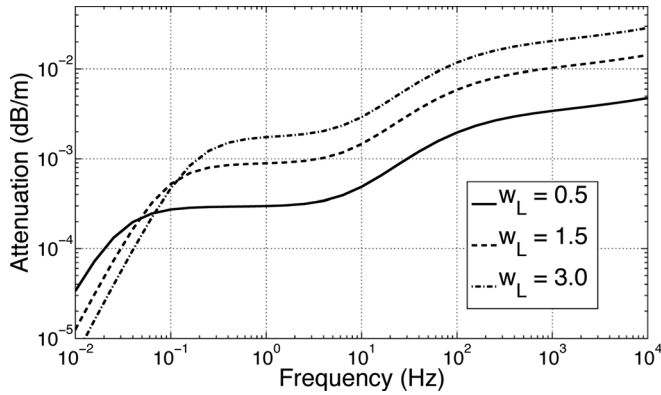


FIG. 4. Influence of water content on absorption by clouds.

extent, so that in the very low frequency range (around 0.01 Hz) the inverse phenomenon is observed: clouds with low water content tend to absorb more infrasound.

The average radius of clouds droplet largely depends on the development stage of the cloud. It can evolve from 5 μm for early stage ones to 40 μm for rainy clouds. For a given water mass content (here $w_L = 1 \text{ g/m}^3$), and when increasing the droplet radius a_0 , the total surface of droplets decreases. Since transfers responsible for absorption effects are surface processes, so does the absorption coefficient, see Fig. 5. However, since all characteristic frequencies f_{pc} and f_v are inversely proportional to the square of the droplet radius, the peak of absorption per wavelength is shifted to low frequencies when the droplet radius increases. This results in an inversion of the dependence of the wave attenuation with radius for the lowest frequencies.

Polydispersion plays a significant role as illustrated by Fig. 6 where the monodispersed case (with constant radius $a = 10 \mu\text{m}$) is replaced by a droplet distribution Eq. (1) with the same mean radius $a_0 = 10 \mu\text{m}$. There are significant changes when comparing the monodispersed and polydispersed cases. Taking into account only a mean radius tends to overestimate the absorption, because the influence of large droplets is underestimated and the total surface of droplets is overestimated. Hence a better equivalent mean radius can be defined:¹⁶

$$a_{31} = \left[\frac{\int a^3 N(a) da}{\int a N(a) da} \right]^{1/2}, \quad (22)$$

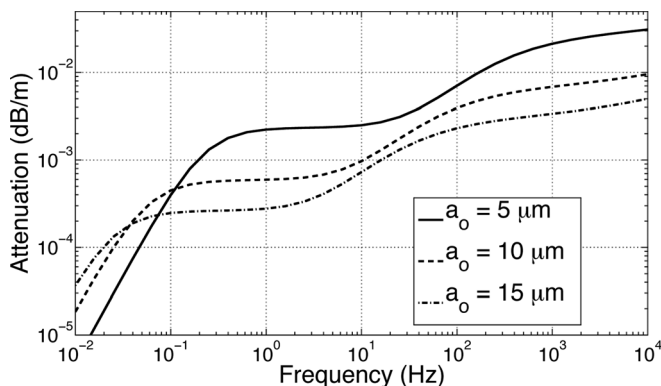


FIG. 5. Influence of droplet radius on absorption by clouds.

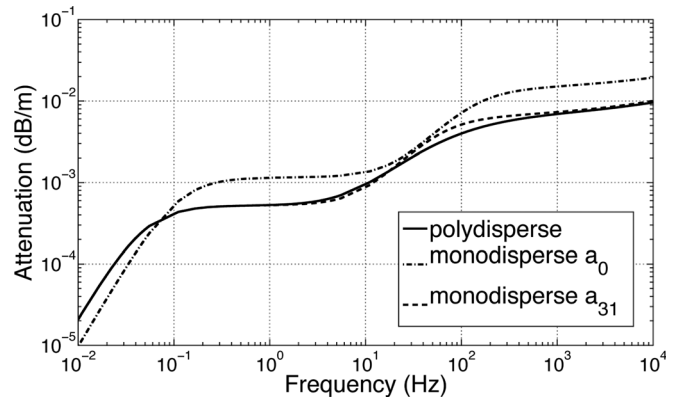


FIG. 6. Influence of polydispersion on absorption by clouds.

based on a mean *surface* defined as the mean volume divided by the mean radius. A much better fit between the polydisperse case and the monodisperse case is then obtained. The same conclusion can be drawn when observing the phase velocity dispersion curves (not shown).

Finally, the influence of altitude is examined on Fig. 7, varying it from 150 to 4000 m, with atmospheric conditions corresponding to ICAO standard atmosphere. When increasing the altitude, the temperature decreases from 14 $^{\circ}\text{C}$ to $-11 \text{ }^{\circ}\text{C}$ and the pressure from 1013 to 616 hPa. The magnitude of the attenuation induced by phase changes depends on the concentration of vapor k_v , while its characteristic frequency depends on the value of the mass fraction m and the diffusion coefficient D (if the droplet radius remains constant). When the altitude is increased, the diffusion coefficient and mass concentration vary about 9% and 33%, respectively, while the vapor concentration is decreased by a factor 5. As a consequence, while the characteristic frequency of phase change f_{pc} is slightly increased, the dominant effect at low frequencies is a diminution of the attenuation induced by phase change (related to the diminution of vapor concentration). At higher frequencies (above 10 Hz), the dominant absorption mechanisms are momentum and heat transfers whose magnitude depends on the mass fraction m . Thus, the increase of the mass ratio with altitude results in an increase of the attenuation above 10 Hz. We can also note that the characteristic frequency of momentum exchange is little affected by the altitude. Anyway, the

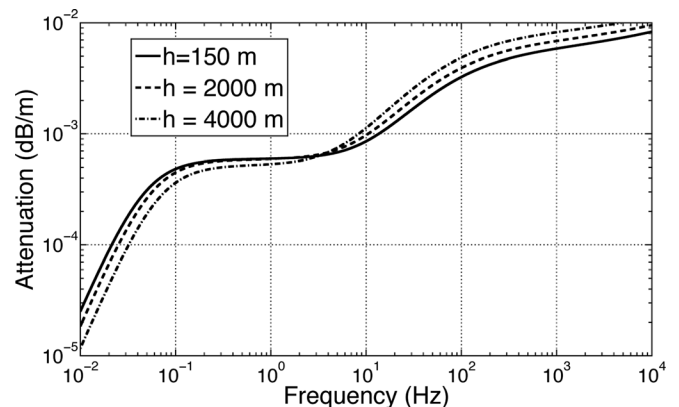


FIG. 7. Influence of altitude on absorption by clouds.

sensitivity of the absorption coefficient to altitude/temperature remains much smaller than sensitivity to other physical parameters.

C. Comparison with standard absorption

Figure 8 compares for various types of clouds the absorption coefficient, computed at the cloud's average altitude according to Table I. Maximum values of water content have been chosen. The resulting absorption is compared to the standard³¹ absorption in humid air without clouds, computed at an altitude of 2000 m and a relative humidity of 100%, just prior to condensation. Even though altitudes are not constant, the comparison remains nevertheless significant as either standard or cloud absorption are not deeply modified by altitude (as shown by Fig. 7) in the considered range. Clearly visible on Fig. 8 is the fact that the coefficient of absorption is quite variable with the type of clouds. In the frequency range 1 to 100 Hz, the clouds with the highest water content (such as cumulonimbus or cumulus at intermediate or final stage) tend to be more efficient sound absorbers. At lower frequencies (around 0.1 Hz), influence of droplet radius is more sensitive, and sound absorption in fogs becomes comparable. At very small frequencies (0.01 Hz), variability with clouds is not very large. In magnitude orders, the coefficient of absorption varies from around 4×10^{-5} dB/km at the lowest frequency (0.01 Hz), to around 2×10^{-3} at 100 Hz, e.g., a change of almost two decades in magnitude for four decades in frequency. However, the most important result is that, when compared to standard absorption, absorption within clouds is much larger up to 100 Hz. It is about ten times more important at 100 Hz, hundred times more at 10 Hz and several decades for lower frequencies. When comparing with standard absorption at lower humidities (20% relative humidity) the conclusion is similar although the discrepancy is slightly smaller because standard absorption is larger for dry air. Note the standard absorption gets dominant over the one due to clouds only above 1000 Hz, while the two are comparable in the frequency range 100 to 1000 Hz. This points out one of the main limitation of the cloud model, that is based on a perfect gas assumption for air. Molecular relaxation of diatomic molecules of nitrogen and oxygen is not taken into account, while it is the

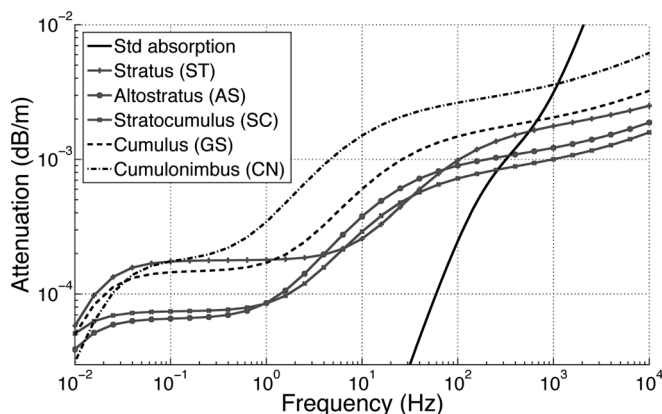


FIG. 8. Comparison of cloud and standard sound absorption.

dominant source of bulk sound absorption up to the MHz range in air without liquid water. Below 100 Hz, the present model is sufficient because droplet absorption is by far dominant. Above 1000 Hz, standard absorption is dominant and droplet influence is negligible. In the intermediate range 100–1000 Hz, both are comparable and the model would need to include real gas effects.

V. APPLICATION TO SONIC BOOM

Locally, sound absorption within clouds is much larger than standard absorption for frequencies below 100 Hz. Nevertheless, one could argue that, anyway, clouds have only a finite thickness and occupy only a small volume of the atmosphere where sound and infrasound propagate. So the question still remains whether absorption by clouds is really important. Of course, the answer may depend on the type of source, its altitude, frequency range and location relative to clouds and receiver. We here investigate one particular case. A sonic boom is a wideband signal, with main frequency spectrum in the 1 to 10 Hz range but with significant content up to typically 100 Hz. Its source, a supersonic aircraft, is located at high altitudes, well above the cloud, but induces some annoyance at the ground level. It is likely to encounter all types of meteorological situations, with or without clouds. Some flight tests performed in the former Soviet Union on Tu144 indicate a significant effect, with reports³⁵ on the perception of a loud sonic boom completely modified in presence of thick clouds. To quantify this effect more precisely, we consider a sonic boom emanating from an aircraft flying in steady flight at Mach 1.6 and 15 km altitude. The source signal is the Whitham function³⁶ associated to a parabolic fuselage 45 m in length, with a volume of 141.3 m³ and a maximum diameter of 1.4 m. This source has already been used as a reference source for investigating the influence of meteorological variability on sonic boom.³⁷ It produces at the ground level and in the standard atmosphere without any absorption an ideal N-wave of amplitude 56 Pa and duration 150 ms. This is typical for the sonic boom of a small supersonic aircraft like a business jet or military fighter (without any low boom design). More realistic sources in terms of aerodynamics lead to identical conclusions about the effect of clouds on sonic boom.

Numerical simulations are performed for ICAO standard atmosphere,²³ with the typical relative humidity profile given by the ISO standard.³¹ Within the thickness of the selected cloud, that humidity profile has been replaced by a 100% relative humidity. Among values of Table I, the minimal value of height h and the maximal value of the water content w_L are chosen. However, for cumulonimbus, the top of the cloud has been limited to 4000 m, since the model is limited to lower altitudes because of the predominant ice content above. Note the resulting meteorological data may not be fully consistent from a meteorological point of view, as formation of a given type of cloud may be associated to some specific meteorological conditions. However, the point here is to evaluate the importance of clouds on sonic boom absorption, not to provide a fully realistic study of sensitivity of sonic booms to cloudy meteorology.

Numerical simulation is based on a process already described and validated in Ref. 37. Sonic boom is computed through a ray tracing approach. Only the ray emitted perpendicular to the Mach cone at a 0° azimuthal angle in the vertical plane of the aircraft trajectory is considered. Along a given ray, the pressure field satisfies Burgers' equation, augmented with ray-tube area variations for geometrical effects, and linear dispersion and absorption. Standard absorption³¹ is considered outside the cloud, and the present model inside the cloudy layer. The cloud is assumed to be a horizontal layer of infinite extent, so that diffraction effects at the edges of the cloudy layer are not considered. The numerical procedure involves a split-step approach. Geometrical effects are taken into account analytically by introducing a linear transformation of the model equation. Nonlinear effects are solved through a quasianalytical shock fitting method³⁸ based on Poisson solution of the inviscid Burgers' equation. Linear dispersion and absorption are solved numerically in the frequency domain. A second-order Strang split-step is chosen to improve convergence. The problem is voluntarily overdiscretized from a numerical point of view, in order to guarantee numerical convergence. Time pressure waveforms are discretized with 2^{15} points, corresponding to a time step of $7\mu\text{s}$, more than 100 times smaller than the actual rise time. The number of spatial steps along the ray is 200, while convergence is generally obtained for values around 30 (thanks to the second-order split-step).

Figure 9 displays the ground pressure waveform when no absorption is considered, for the standard absorption only (no cloud), and for five different clouds. Pressure signal is zoomed on the head shock, to better view the shock structure resulting from the various absorption and dispersion effects. Table II summarizes the main characteristic of the ground pressure field for seven different clouds: (1) peak overpressure (in Pa), (2) rise time (in ms) of the head shock (time necessary for the pressure waveform to go from 10% to 90% of the peak overpressure), and (3) Sound Exposure Level (SEL) with two different frequency A- and C-weightings. ASEL metric is considered (along with Perceived Level) as the best metric for measuring the human response to sonic boom heard outdoor in laboratory conditions.³⁹ C-weighting is frequently recommended for estimating the human response to loud impulsive noises.⁴⁰ In general, standard absorption and clouds tend to preserve the general "N-like" shape of the boom, but reduce the peak overpressure and make shocks smoother. Compared to standard atmosphere,

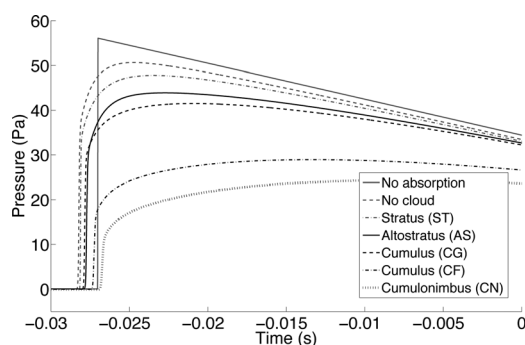


FIG. 9. Sonic boom attenuation by clouds: head shocks.

TABLE II. Sonic boom absorption by atmospheric clouds.

Type	P_{\max} (Pa)	t_m (ms)	SEL (dBA)	SEL (dBC)
No absorption	56.08	0.007	94.48	105.90
No cloud	50.63	0.869	90.58	104.98
Stratocumulus	48.03	0.762	90.50	104.56
Fog	47.78	1.073	90.21	104.42
Altostratus	43.89	1.116	88.82	103.61
Cumulus				
Early stage	47.61	1.159	89.63	104.36
Growing stage	41.50	1.341	88.52	103.15
Final stage	28.92	4.024	83.41	98.88
Cumulonimbus	24.31	7.029	80.40	96.48

clouds tend to amplify this effect. The effect is moderate for thin cloud (fog or altostratus) but is very significant for thick clouds (cumulus at final stage or cumulonimbus). In the last case, the peak overpressure is more than halved compared to the standard case. Indeed, sound absorption in clouds is much more efficient than standard absorption at frequencies corresponding to the peak of the boom spectrum (1 to 10 Hz). While standard absorption barely affects this part of the boom spectrum, cloud absorption does. The effect is small for thin clouds because propagation path is too short (500 m vertically for fog), but large for thick clouds (4000 m for cumulonimbus). The nonzero value ($7\mu\text{s}$) of the rise time in the nonabsorbing case is due to the finite time discretization, with the head shock spread over two grid points only. Rise time in the standard case (no cloud) is on the order of 0.8 ms. Clouds systematically increase that rise time. That increase is almost insignificant for fog, but once again very large for thick clouds. When examining overall sound exposure levels, one again observes a decrease compared to the standard case, in any metric. That effect is almost insignificant for thin clouds (on the order of 0.5 dB for fog), but is extremely large for thick clouds (more than 10 dB for cumulonimbus and A-weighting, 8.5 dB for C-weighting).

VI. CONCLUSION

This study examines and quantifies the influence of atmospheric clouds on propagation of sound and infrasound. Two main limitations of an existing model¹⁶ have been outlined. First, it is limited to temperatures higher than about -10°C . For colder conditions, the ice content would be too large and a four phase model (air, vapor, liquid water, and ice) would be necessary. Second, the assumption of perfect gases neglects relaxation effects associated to the diatomic nature of nitrogen and oxygen molecules. This effect gets predominant compared to droplet effects within clouds for frequencies over 1000 Hz, and the present model is applicable only for frequencies lower than 100 Hz. In this frequency range, absorption by clouds turns out to be one or several magnitude orders larger than standard absorption. The model shows that phase change effects are predominant at low frequencies (below 1 Hz), while steady thermal and viscous drag is the leading effect above 10 Hz. Unsteady effects are negligible in the considered frequency range. Even though the value of the evaporation parameter is pretty uncertain,

the overall absorption is anyway almost insensitive to this parameter. This is explained by the fact that phase changes are limited by the diffusion of vapor in air. Sound absorption in clouds is mostly sensitive to the radius of water droplets and the total water content. For frequencies above 0.01 Hz, clouds with small droplets and high water content absorb more because they maximize the total surface of droplets. Sound absorption in clouds is much less sensitive to altitude. Dispersion in droplet radii is important to take into account. It can be estimated with a good accuracy by considering an adequate mean radius. Application to sonic boom shows that clouds decrease the peak overpressure, increase the rise time of the head shock and decrease the noise level. That effect is small for short propagation paths within clouds (a few hundred meters) but can be very large for thick clouds (several kilometers). Further work would require to improve the model: include real gas effects, and take into account the presence of ice for high altitude clouds. Other applications could consider other types of low frequency or infrasonic

sources. Use of database where cloud data is consistent with other meteorological parameters could also be contemplated.

ACKNOWLEDGMENT

This study was supported by Airbus Operations SAS.

APPENDIX: DISPERSION RELATION

From expressions of Sec. III B, the dispersion relation is obtained for a plane harmonic wave of complex wave number $k(\omega)$ under the form $k = (\omega/c_{go})\sqrt{V(\omega)D(\omega)}$ with c_{go} the sound speed in the gaseous phase (air + vapor), $V(\omega)$ the contribution of momentum transfers and $D(\omega)$ the one of thermal transfers and phase change. Expressions of $V(\omega)$ and $D(\omega)$ are given below as a function of parameters and characteristic times introduced in Sec. III B. Both terms $V(\omega)$ and $D(\omega)$ are of the form $1 + m \dots$, as effects induced by the presence of droplets are directly proportional to the mass concentration m (dilute approximation):

$$\begin{aligned}
 V(\omega) &= 1 + m \frac{(\alpha_{go} - r_o)\langle h_F \rangle_a - \alpha_{go} r_o}{1 + m r_o \langle h_F \rangle_a}, \\
 D(\omega) &= 1 + m(\gamma_{go} - 1) \frac{\langle h_{T2} \rangle_a - \bar{R}_v k_{vo} \gamma_{go} (\bar{R}_v \bar{C}_{go}^p \langle h_{T3} \rangle_a - 2 \bar{l}_o r_o \langle h_{T1} \rangle_a - M_1 \Lambda)}{1 + m (\langle h_{T2} \rangle_a - B \langle h_{T3} \rangle_a - M_2 \Lambda)}, \\
 \Lambda &= r_o L \langle h_{T1} \rangle_a^2 + \langle h_{T2} \rangle_a \langle h_{T3} \rangle_a, \quad \bar{R}_v = \frac{R_v}{R_{go}}, \quad \bar{l}_o = \frac{l_o}{c_{go}^2}, \quad \bar{C}_{go}^p = \frac{C_{go}^p}{\gamma_{go} R_{go}} = \frac{1}{\gamma_{go} - 1}, \quad \bar{C}_{lo} = \frac{C_{lo}}{\gamma_{go} R_{go}}, \\
 h_F &= (1 - \tau_v^* / \tau_A^*) / (1 - i \omega \tau_v^*), \quad h_{T1} = Z e_2, \quad h_{T2} = Z(e_1 - L e_2), \quad h_{T3} = Z e_2 (r_o - i \omega \tau_{\Sigma_g}^* e_1), \\
 B &= (1 - \bar{R}_v k_{vo}) \bar{R}_v, \quad L = r_o \gamma_{go} (\gamma_{go} - 1) k_{vo} \bar{l}_o^2, \quad M_1 = m \bar{R}_v \bar{C}_{go}^p (\gamma_{go} - 1 + \bar{R}_v k_{vo}), \quad M_2 = m B, \\
 Z &= r_o / [r_o - i \omega \tau_{\Sigma_g}^* (e_1 - \rho_{vo} r_o \bar{l}_o (\gamma_{go} - 1) e_2) / p_{go}], \quad e_1 = (C_{lo} / C_{go}^p) (1 - i \omega \tau_{T1}^*)^{-1}, \quad e_2 = (i \omega (\tau_D^* + \tau_\beta))^{-1}. \quad (A1)
 \end{aligned}$$

Note that we found a few differences with expressions from Ref. 16 First, we find a coefficient 1/15 instead of 1/3 in the expression of τ_{T1}^* . Second, in the expression of τ_β , we have $\sqrt{2\pi/\gamma_{vo}}$ instead of $\sqrt{2\pi/\gamma_{vo}}$. Finally we have $l_o \bar{l}$ instead of l_o , in the expression of Z .

¹C. J. T. Sewell, "On the extinction of sound in a viscous atmosphere by small obstacles of cylindrical and spherical form," *Philos. Trans. R. Soc. London* **210**, 239–270 (1910).

²H. Lamb, *Hydrodynamics* (Dover, New York, 1945), pp. 659–661.

³M. A. Isakovich, "On the propagation of sound in emulsions," *Zh. Exp. Teor. Fiz.* **18**, 907–912 (1948).

⁴P. S. Epstein and R. R. Carhart, "The absorption of sound in suspensions and emulsions. I. Waterfog in air," *J. Acoust. Soc. Am.* **25**, 553–565 (1953).

⁵J. R. Allegra and S. A. Hawley, "Attenuation of sound in suspensions and emulsions: Theory and experiments," *J. Acoust. Soc. Am.* **51**, 1545–1564 (1972).

⁶A. Viglin, "Propagation of vibrations in a two-phase vapour-liquid system," *Zh. Tekh. Fiz.* 275–285 (1938).

⁷K. von Oswatitsch, "Die Dispersion und Absorption des Schalles in Wolken (Sound dispersion and absorption in clouds)," *Phys. A* **42**, 365–378 (1941).

⁸F. E. Marble, "Dynamic of dusty gases," *Ann. Rev. Fluid Mech.* **2**, 397–446 (1970).

⁹F. E. Marble and D. C. Wooten, "Sound attenuation in a condensing vapor," *Phys. Fluids* **13**, 2657–2664 (1970).

¹⁰J. E. Cole and R. A. Dobbins, "Propagation of sound through atmospheric fog," *J. Atmos. Sci.* **27**, 426–434 (1970).

¹¹A. I. Ivandaev and R. I. Nigmatulin, "On the propagation of weak perturbations in two phase media with phase transformations," *Zh. Prikl. Mekh. Tekh. Fiz.* **5**, 73–77 (1970).

¹²J. Barrett and C. Clement, "Kinetic evaporation and condensation rates and their coefficient," *J. Colloid Interface Sci.* **150**, 352–364 (1992).

¹³I. W. Eames, N. J. Marr, and H. Sabir, "The evaporation coefficient of water: a review," *Int. J. Heat Mass Transfer* **40**, 2963–2973 (1997).

¹⁴R. W. Schrage, *A Theoretical Study of Interphase Mass Transfer* (Columbia University Press, New York, 1953), pp. 25–43.

¹⁵N. A. Gumerov, A. I. Ivandaev, and R. I. Nigmatulin, "Sound waves in monodisperse gas-particle or vapour-droplet mixtures," *J. Fluid Mech.* **193**, 53–74 (1988).

¹⁶R. A. Gubaidullin and R. I. Nigmatulin, "On the theory of acoustic waves in polydispersed gaz-vapor-droplet suspensions," *Int. J. Multiphase Flow* **26**, 207–228 (2000).

¹⁷R. Duraiswami and A. Prosperetti, "Linear pressure wave in fogs," *J. Fluid Mech.* **299**, 187–215 (1995).

¹⁸V. O. Knudsen, J. V. Wilson, and N. S. Anderson, "The attenuation of audible sound in fog and smoke," *J. Acoust. Soc. Am.* **20**, 849–857 (1948).

¹⁹R. A. Dobbins and S. Temkin, "Measurement of particulate acoustic attenuation," *AIAA J.* **2**, 1106–1111 (1964).

²⁰S. Temkin and R. Dobbins, "Attenuation and dispersion of sound by particulate-relaxation processes," *J. Acoust. Soc. Am.* **40**, 317–324 (1966).

- ²¹J. E. Cole and R. A. Dobbins, "Measurement of the attenuation of sound by a warm air fog," *J. Atmos. Sci.* **28**, 202–209 (1971).
- ²²H. R. Pruppacher and J. D. Klett, *Microphysics of Clouds and Precipitation* (Kluwer Academic, Dordrecht, 1978), pp. 26–27, 39, 87, 93, 116, 503, 854.
- ²³ICAO, "Manual of the ICAO standard atmosphere (extended to 80 km)," Technical Report, ICAO, Doc 7488-third edition (1993).
- ²⁴M. Ishii and T. Hibiki, *Thermo-Fluid Dynamic Theory of Two-Phase Flow* (Springer, New York, 2006), pp. 93–117.
- ²⁵Y. A. Buyevich and I. N. Shchelchkova, "Flow of dense suspensions," *Prog. Aerospace Sci.* **18**, 121–151 (1978).
- ²⁶Y. A. Buyevich and V. G. Markov, "Rheology of concentrated mixtures of fluids with small particles," *PMM* **36**, 480–493 (1972).
- ²⁷National Institute of Standards and Technology, "Webbook of Chemistry," <http://webbook.nist.gov/chemistry> (Last viewed 22 July 2011).
- ²⁸M. Baudoin, J.-L. Thomas, and F. Coulouvrat, "On the influence of the particles correlations in position on the sound propagation in concentrated solutions of rigid particles," *J. Acoust. Soc. Am.* **123**, 4127–4139 (2008).
- ²⁹M. Baudoin, J.-L. Thomas, F. Coulouvrat, and D. Lhuillier, "An extended coupled phase theory for the sound propagation in polydisperse suspensions of rigid particles," *J. Acoust. Soc. Am.* **121**, 3386–3397 (2007).
- ³⁰H. E. Bass, L. Sutherland, J. Piercy, and L. Evans, "Absorption of sound by the atmosphere," in *Physical Acoustics: Principles and Methods*, (Academic, Orlando, 1984), Vol. XVII, pp. 145–232.
- ³¹ISO 9613-1 "Acoustics - Attenuation of sound during propagation outdoors - part 1: Calculation of the absorption of sound by the atmosphere," International Organization for Standardization, Genève (1993).
- ³²M. Baudoin, J.-L. Thomas, F. Coulouvrat, and C. Chanéac, "Scattering of ultrasonic shock waves in suspensions of silica nanoparticles," *J. Acoust. Soc. Am.* **129**, 1209–1220 (2011).
- ³³L. D. Landau and E. M. Lifshitz, *Course of Theoretical Physics. Vol. 6. Fluid Mechanics*, 2nd ed. (Butterworth-Heinemann, Oxford, 1987), p. 254.
- ³⁴A. Perelomova, "A small-signal sound speed and parameter of non-linearity B/A in a ternary mixture. Examples on calculations of mixture consisting of air, water and water vapour," *Acta Acust. Acust.* **91**, 809–816 (2005).
- ³⁵V. S. Gratchev, Y. A. Zaverchnev, A. D. Ivanov, I. A. Mironov, and A. V. Rodnov, "Experimental study of the influence of turbulence and nebulosity on sonic boom," Technical Report, ONERA (incomplete French translation of a Soviet report in Russian without reference) (1966).
- ³⁶G. B. Whitham, "The flow pattern of a supersonic projectile," *Commun. Pure Appl. Math.* **5**, 301–348 (1952).
- ³⁷A. Loubeau and F. Coulouvrat, "Effects of meteorological variability on sonic boom propagation from hypersonic aircraft," *AIAA J.* **47**, 2632–2641 (2009).
- ³⁸F. Coulouvrat, "A quasi exact shock fitting algorithm for general nonlinear progressive waves," *Wave Motion* **49**, 97–107 (2009).
- ³⁹J. D. Leatherwood, B. M. Sullivan, K. P. Shepherd, D. A. McCurdy, and S. A. Brown, "Summary of recent NASA studies of human response to sonic booms," *J. Acoust. Soc. Am.* **111**, 586–598 (2002).
- ⁴⁰CHABA, "Community Response to High-Energy Impulsive Sounds: An Assessment of the Field Since 1981," *Committee on Hearing, Bioacoustics and Biomechanics (CHABA)* (National Academy Press, Washington, DC, 1996), pp. 20–21.